A comparison of a first-order thermal lensing model to a closed aperture Z-scan for the propagation of light in ocular media.

Rebecca L. Vincelette[a,b], Robert J. Thomas[a], Benjamin A. Rockwell[a], Ashley J. Welch[b]
[a]USAF Research Laboratory, 2624 Louis Bauer Dr., Brooks City-Base, TX, 78235-5278
[b]University of Texas in Austin, Department of Biomedical Engineering, 1 University Station C0800, Austin, TX, 78712

ABSTRACT

The phenomenon of thermal lensing was investigated in water using a Z-scan method and corresponding first-order mathematical models. Data from first-order thermal lensing models and ABCD beam propagation methods were used to simulate the non-linear absorption of water held in a thin sample cuvette for a Z-scan optical set up of CW cases at 1313 nm. The single beam closed aperture Z-scan was then used to determine the non-linear absorption at 1313 nm for water in 10 mm and 2 mm cuvettes at 48.00, 16.80, 9.80 and 2.83 mW then compared to the first-order model data. The results from the closed aperture Z-scan were also used to back calculate the spot size in the far field for comparison to the model's prediction of the beam's temporal response. Experimental Z-scan data were found not to correlate strongly with our first-order model suggesting the need for higher order models to successfully predict spot size in absorbing media inside the Rayleigh range.

Keywords: Thermal Lensing, Thermal Damage Models, Optical Radiation, Retinal Damage Model, Z-Scan

1. INTRODUCTION

Damage thresholds are important for providing safety guidelines in the American National Standards Institute, ANSI.[1] As a result, these safety guidelines are used in areas which employ the use of laser technology. For example, retinal laser surgeries are used to treat ocular disorders such as macular edema and central serous retinopathy by coagulating small areas of abnormal microvascular activity.[2, 3] Predicting safe exposure levels and subsequent damage thresholds for pulsed or continuous wave, CW, lasers for treatment wavelengths at a given power require knowledge about the spot size of the beam on the retinal plane. If beam parameters such as spot size and power at the retina are known then a damage threshold can be derived based on tissue properties and the fluence rate on the retina.[4, 5] It is hypothesized that thermal lensing within the human eye yields a significant amount of change in beam geometry impacting the resulting damage threshold value for a variety of spot size conditions.

Thermal lensing is a well known phenomenon in analytical chemistry where a temperature gradient, ΔT, forms in an absorbing media resulting in a change in density, ρ, of the material where absorption occurred leading to the change in index of refraction, n, with respect to temperature.[6, 7, 8] This effect yields a thermo-optic coefficient represented mathematically as dn/dT. Whenever the index of refraction changes, the path the beam takes through the media is altered from the original path resulting in a shift in focus. In media which exhibit a decrease in density as temperature increases, such as ocular tissue, the index of refraction decreases with respect to the temperature rise, a negative dn/dT, resulting in a negative lens like effect also known as thermal blooming.[7] A negative lens effect would also mean the focal point would shift behind the original focal plane.

The long term research goals in this area are to develop thermal lensing models for ocular media derived from earlier thermo-optic models developed for solid state optics research. [9, 10, 11] These adapted thermal lensing models will be compared to experimental data for both thick and thin samples for validation, then used to provide information to retinal damage models created by Thomas et al. in 2003.[4, 12] Ultimately, this research will impact the way in which predictions and assessments for damage on the retina are made in order to provide critical information to the medical community for eye surgeries and retinal imaging techniques which utilize laser technologies. In this study, a first-order thermal lensing model was created in LabVIEW™ (National Instruments) to simulate the thermal lensing properties of the human eye. First-order model data were compared to experimental data collected using a single-beam closed aperture Z-scan set up.[6]

Optical Interactions with Tissue and Cells XVII, edited by Steven L. Jacques, William P. Roach,
Proc. of SPIE Vol. 6084, 60840G, (2006) · 1605-7422/06/$15 · doi: 10.1117/12.645445

2. METHODOLOGY

2.1 First-order model

In the 1960's, Gordon et al.[8] discovered as media absorbs energy, the pathlength of light through a media changes, resulting in changes of a beam profile within a sample. Gordon et al.'s [8] discovery became known as thermal blooming or thermal lensing since many media exhibited characteristics of broadening the beam upon exposure to light energy. To successfully model thermal lensing, time dependent terms for describing both thermal effects and beam geometry within a sample must be determined.[9, 10, 11]

As a media absorbs energy, physical characteristics such as density and temperature change. These physical changes impact the index of refraction, n. Van Stryland et al.[11] describe n in terms of the change in density, ρ, and temperature T by a term for the thermal expansion, $\partial n / \partial \rho$ and a term for other temperature changes, $\partial n / \partial T$. The term for thermal expansion is commonly referred to as electrostriction.

$$\Delta n = \left(\frac{\partial n}{\partial \rho}\right)_T \Delta \rho + \left(\frac{\partial n}{\partial T}\right)_\rho \Delta T \qquad (1)$$

The electrostriction component can be approximated by a constant if the time it takes for an acoustic wave to travel the distance of the minimum beam spot is less than the time of the pulse width or pulse on time, τ.[11] This would hold true for cases involving long pulse durations or continuous wave, CW. This simplifies Eq. 1 to the thermo-optic effect in Eq. 2.

To consider the thermal effects for the first-order model a Gaussian beam in TEM_{00} mode was assumed to propagate through an absorbing media where the temperature along the beam path would be greatest in the center and coolest at the outer edge of the beam profile. This would mean the index of refraction in areas at higher temperatures would be lower than the index of refraction in areas of cooler temperatures, ultimately describing how a media can exhibit a negative lens like behavior. The thermal profile within an absorbing media was described by the radius, $\vec{r}$, from the optical axis, position, z, along the optical axis, and time, t, resulting in Eq. 2.[9, 10]

$$n(\vec{r}, z, t) = n_o + \left(\frac{\partial n}{\partial T}\right)_\rho T(\vec{r}, z, t) \qquad (2)$$

Where n_o is the background index of refraction. Electrostriction was neglected for the purposes of this study as pulse widths were greater than the acoustic transit times for all cases represented here.

The mathematical model used for the thermal lensing effect originates from the Green's Function solution to the thermal diffusion equation (Eq. 3). [13]

$$\nabla^2 T(\vec{r}, t) - \frac{1}{\eta}\frac{\partial T(\vec{r}, t)}{\partial t} = -4\pi S(\vec{r}, t) \qquad (3)$$

Where T is temperature, t is time, $\vec{r}$ is the radial vector, η is the thermal diffusivity, and S is the source term.

Assuming a cylindrical symmetric medium where diffusion along the optical axis is zero ($\partial z / \partial T = 0$), then the solution to the diffusion equation at radius, $\vec{r}$ and time, t, can be described by [9]

$$G(\vec{r}, t; \vec{r}', t') = -\frac{1}{4\pi(t - t')} \exp\left[-\frac{|\vec{r} - \vec{r}'|}{4\eta(t - t')}\right] \qquad (4)$$

Where $G(\bar{r},t;\bar{r}',t')=0$ for all positions where $\bar{r}$ is on the surface of the cylindrical media and $G(\bar{r},t;\bar{r}',t')=0$ for all times, t < t'.

The temperature rise in the medium at position $\bar{r}$ can be determined by integrating over all $\bar{r}'$ in the medium.[10] In order to accurately represent the accumulating thermal effects of a continuously pulsed or chopped source, the temperature rise in the media will be related to the current pulse and any residual contributions from previous pulses.[10]

$$T(\bar{r},t_m;m)=\int_0^{t_m}dt'\int_0^{\infty}d\bar{r}'S(\bar{r}')G(\bar{r},t;\bar{r}',t')+\sum_{n=1}^{m-1}\int_{A_n}^{A_n+\tau}dt'_n\int_0^{\infty}d\bar{r}'S(\bar{r}')G(\bar{r},t;\bar{r}',t'_n) \quad (5)$$

Where t_m is the time during the m^{th} on pulse. $A_n=(t_m+\tau')+(n-1)(\tau+\tau')$ with τ = on time and τ' = off time.
The temperature change for when the pulse is off can then be described by the events following the m^{th} pulse by Eq. 6.

$$T(\bar{r},t'_m;m)=\sum_{n=1}^{m}\int_{C_{mn}}^{C_{mn}+\tau}dt'_n\times\int_0^{\infty}d\bar{r}'S(\bar{r}')G(\bar{r},t;\bar{r}',t'_n) \quad (6)$$

Where $C_n=t'_m+(n-1)(\tau+\tau')$. Fig. 1 depicts the timing diagram.

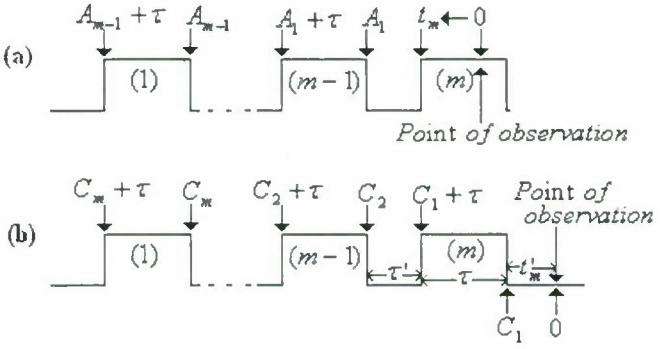

Figure 1: The timing diagram used in the thermal lensing model for m pulses with on time, τ, and off time, τ'. (a) and (b) depict the sequences used for when the observation point is taken when the pulse is on and off respectively. Note the point of observation is actually the zero point in time. Equations for A_n and C_n are described in Eq. 5 and 6. t_m is the time from the last rising edge of the most recent on pulse to the point of observation and t_m' is the time from the last falling edge of the most recent on pulse to the point of observation taken while the pulse is off. (Figure adapted from Swofford et al.)[10]

Using the formulism by Fang and Swofford, Eq. 2 can be re-written as [10]

$$n(r,T)=n(0,T)+\frac{1}{2}r^2\left(\frac{\partial n}{\partial r}\right)\left(\frac{\partial^2 T}{\partial r^2}\right)_{r=0} \quad (7)$$

To describe the temporal dependency for the thermal response, an expression for the source term can be found by applying Beer's law for the heat generated from absorption per unit length through the sample and assuming a Gaussian beam.[9, 10]

$$S(r,t)=\frac{2\mu_a}{\pi\omega^2\kappa}\exp\left[\frac{-2(\bar{r})^2}{\omega^2}\right]P_o(t) \quad (8)$$

Where μ_a is the linear absorption coefficient, ω is the $1/e^2$ beam radius, κ is the thermal conductivity and $P_o(t)$ is the power as a function of time, t. Cases using a square pulse can allow $P_o(t)$ to be a constant.

Cases involving one or more square temporal pulses can be written in terms of the on and off portions of the pulse shown in Eq. 9 and 10 respectively.

$$\left(\frac{\partial^2 T}{\partial r^2}\right)_{r=0} = \frac{-\mu_a P}{\pi\varpi^2\kappa}\left[\frac{1}{1+\frac{t_c}{2t_m}} + \sum_{n=1}^{m-1}\left(\frac{1}{1+\frac{2A_n}{t_c}} - \frac{1}{1+2\frac{A_n+\tau}{t_c}}\right)\right] \tag{9}$$

$$\left(\frac{\partial^2 T'}{\partial r^2}\right)_{r=0} = \frac{-\mu_a P}{\pi\varpi^2\kappa}\left[\sum_{n=1}^{m-1}\left(\frac{1}{1+\frac{2C_n}{t_c}} - \frac{1}{1+2\frac{C_n+\tau}{t_c}}\right)\right] \tag{10}$$

Where μ_a is the linear absorption coefficient, κ is the thermal conductivity, P is the power when the pulse is on, ω is the $1/e^2$ beam radius (assumed to be constant over a very small increment, Δz), t_m is the time from the last rising edge of the most recent on pulse to the point of observation, τ is the pulse on time, and t_c is the critical time defined by $t_c = \eta/8\omega_o$.

To propagate the Gaussian beam through space, we used the ABCD law.[7, 14] The Gaussian beam is described by a complex number at spatial position, z, with the radius of curvature, R, representing the real portion and the beam radius and wavelength for the imaginary component.

$$\frac{1}{q(z)} = \frac{1}{R(z)} - i\frac{\lambda}{\pi\omega(z)^2} \tag{11}$$

Yariv[7] details how to model a Gaussian beam moving through a diverging lens-like media described by a quadratic index of refraction by the following transformation matrix.

$$\begin{bmatrix} A & B \\ C & D \end{bmatrix} = \begin{bmatrix} \cosh\left(\sqrt{X}\Delta z\right) & \sqrt{X}\sinh\left(\sqrt{X}\Delta z\right) \\ \sqrt{X}\sinh\left(\sqrt{X}\Delta z\right) & \cosh\left(\sqrt{X}\Delta z\right) \end{bmatrix} \tag{12}$$

Where Δz is a small spatial increment along the optical axis and X is defined in Eq. 13.[10]

$$X = \frac{1}{n(0,T)}\left(\frac{\partial n}{\partial T}\right)\left(\frac{\partial^2 T}{\partial r^2}\right)_{r=0} \tag{13}$$

The new complex beam parameter is updated by the previous value of q(z) and the matrix in Eq. 14 by the following relationship.[7]

$$q(z)_{new} = \frac{Aq(z)_{old} + B}{Cq(z)_{old} + D} \tag{14}$$

The solution is found by iteratively calculating the beam radius as a function of spatial position, $\omega(z)$, through the sample using an initial guess for the case of no thermal lensing. This process yields a self-consistent description of $\omega(z)$ at any

observation time, t. The resulting data for $\omega(z)$ can then be used to evaluate the thermodynamic interaction of the beam with the sample.

2.2 Single beam, closed aperture Z-scan experiment

Experimentally characterizing thermal lensing in a media can be accomplished by using the Z-scan method.[6, 15, 16, 17] In a Z-scan, the relative transmittance is read by a photodiode placed behind an aperture as the sample is moved in incremental steps in front, through and behind the depth of focus of a focusing lens. Optical elements such as the focusing lens and neutral density (ND) filers are placed before the chopper in order for any thermal lensing effects within optical elements to reach steady state. Resulting data are measurements of relative beam intensity, related by transmittance detected over the surface area of the photodiode, where a value for dn/dT can be found by determining the best fit to the experimental Z-scan data.

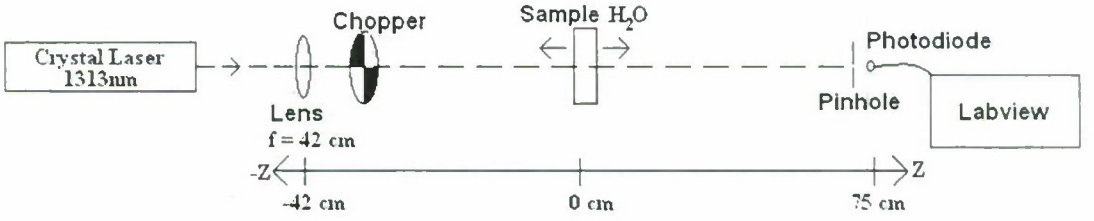

Figure 2: The Z-scan set-up used for the experimental data collection. Sample cuvettes were 2 and 10 mm thick and contained DI H_2O. Positions to the left (in front) of the focal point of the lens are negative and positions to the right (behind) of the focal point are positive. All transmittance values were normalized to the transmittance detected when the sample was placed in the beam path outside the depth of focus of the lens.

In a closed aperture z-scan, the photodiode is placed in the far field, in this case it was placed 117 cm from the pump beam focusing lens. The probe beam transmittance was then normalized relative to the energy detected when the shutter was open and the sample was 70 cm after the focus; a position where no thermal lensing should occur. Upon exposure to the beam, the thermal lensing effect for a negative lens like media will result in an increase and decrease in relative transmittance for cases inside the Rayleigh range before and after the focus respectively. The sample was moved along the z-axis to achieve transmittance readings for various areas within the Rayleigh range. The inflection point is observed at the focus. An example of what closed aperture z-scan data appear as for a negative lens case is shown in Fig. 3 below.

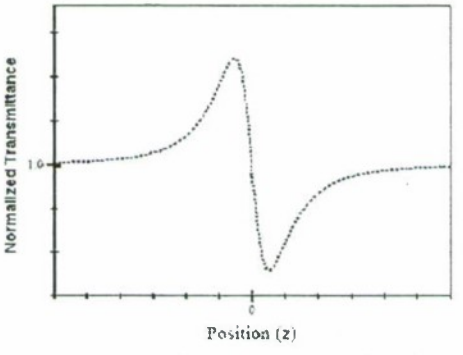

Figure 3: An example of typical data from a closed aperture z-scan. Z-position refers to the position of the sample relative to the focus marked as zero.

A Crystal Laser Model IRCL-150-1313-P-L was used. A Galilean telescope was configured to create a collimated expanded beam with $1/e^2$ diameters of 3.5 mm. A focusing lens of 400 mm made of BK7 glass was used. A knife edge test was conducted to determine the focal position of the lens. The pump beam focusing lens was placed before the chopper to allow for any thermal effects within the BK7 glass to achieve steady state throughout the duration of the experiment.

The sample cuvette containing de-ionized ultra-filtered water was moved along the z-axis by a large micrometer mount. Blank measurements for an empty cuvette were determined to yield no change in normalized transmittance, thus assuring thermal lensing of the cuvette for the pump wavelength was negligible in this experiment.

The power of the beam was lowered by using a Thorlab NEK01 neutral density filter set. When a ND filter of 0.5, 1.0, 2.0 and 3.0 were inserted into the pump path a power of 48, 16.8, 9.8 and 2.83 mW were delivered to the sample respectively. The system was re-aligned each time a new ND filter was added or removed from the optical set up. The photodiode was a United Detector Technology 8028 and was connected to a Melles Griot large dynamic range transimpedance amplifier where the signal was then read into a Labview program. Data were then processed in Matlab to compare to the first order model.

The aperture size was selected to achieve readings between 30-75% of the maximum power read at the selected detector position. The aperture diameter was 2.5 mm for each experiment. The z-positions ran from -18 to 52 cm in incremental steps of 1 cm. The m^2 value for the beam profile was found to be 1.16.

Experimental cases were investigated with the following z-scan parameters summarized in the Tables below.

(a)

Pump wavelength (nm)	Time between exposures (s)	Sampling rate (Hz)	Measured lens focal length (using knife edge) (cm)	$1/e^2$ Beam radius (at lens) (mm)	Distance from lens to detector (cm)	Iris diameter (mm)
1313	20	2500	42	1.74	117	2.5

(b)

Exposure duration (sec)	Sample thickness (mm)	Pump power at sample (mW)	Temperature of room (sample at room temp) (°C)
0.1	2	2.83	18.3
		9.8	17.3
		16.8	16.1
		48	16.1
	10	2.83	18.3
		9.8	17.3
		16.8	16.1
		48	16.1

(c)

Sample thickness (mm)	Exposure duration (sec)	Pump power at sample (mW)	Temperature of room (sample at room temp) (°C)
10	0.5	2.83	18.9
		48	20.6
	1	2.83	18.9
		48	20

Table 1: Single beam closed aperture z-scan experimental parameters in this comparison study. (a) Standard settings used in each experiment conducted. (b) Parameters used for comparison of varying power and sample thickness. (c) Parameters used for comparison of varying exposure duration.

3. DATA & RESULTS

Several studies have been conducted on the linear absorption coefficient for water.[18, 19] For the purposes of this study, the absorption coefficient data from Hale et al.[18] were used to approximate an α for 1313 nm yielding 126 1/m. The value

used for κ was 0.6 J/(msk). Determining a dn/dT for 1313 nm was done by fitting a polynomial to data published by Schiebener et al.[20, 21, 22] The background index of refraction for water at 1313 nm was 1.315 and was assumed to be for an ambient temperature of 25 °C.

The first order model was run for each of the experimental equivalents described in Table 1. The results are shown in Fig's. 4 and 5 below.

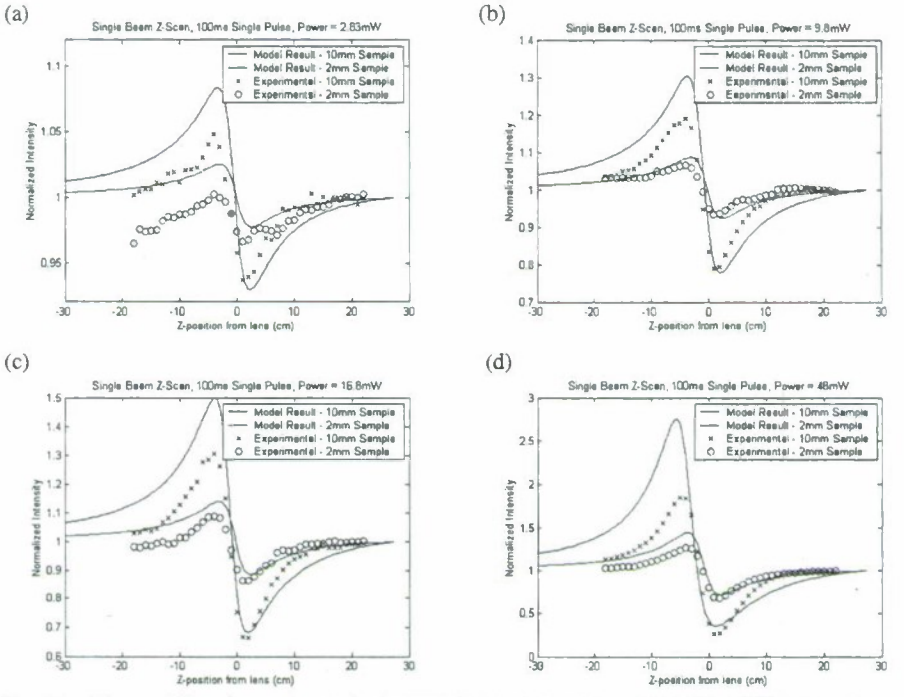

Figure 4: Results of the model and experiment for 2 mm (circles) and 10 mm (x's) with a 100 ms exposure for (a) 2.83 mW, (b) 9.8 mW, (c) 16.8 mW and (d) 48 mW.

Modeling results deviated further from the data as sample thickness increased and power increased. The data for the 2 mm thick sample in Fig. 1(a) was very noisy and difficult to detect even with several scans and multiple averaging techniques. The model seems to fit the 2 mm sample more successfully in three of the four power settings compared to the 10 mm sample.

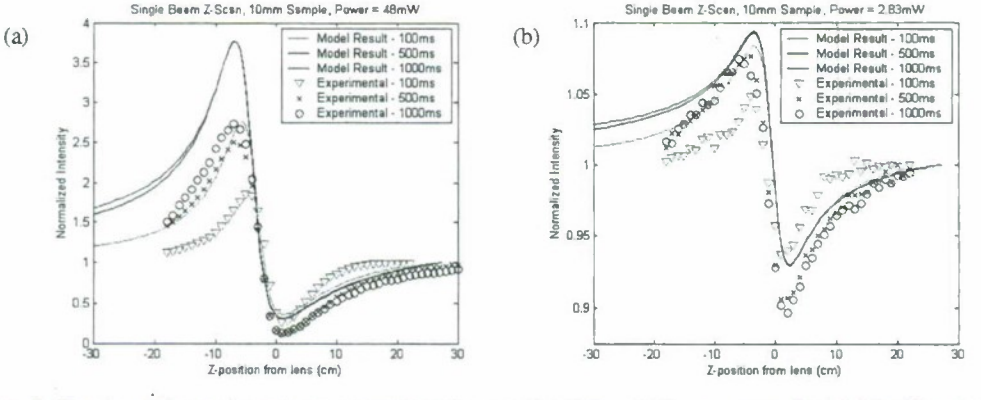

Figure 5: Results of the model and experiment for 10 mm at 0.1, 0.5 and 1.0 s exposures for (a) 48 mW and (b) 2.83 mW.

The modeling results shown in Fig. 5 reflect how the model deviates from the data further as the length of exposure increases. Fig. 5 also illustrates how the model over estimates the thermal lensing effect further as power increases.

4. DISCUSSION

Originally, the model was used to try to find a dn/dT which fit the data. While running simulations with the model, it was discovered small increases in the magnitude of the linear absorption coefficient, α, resulted in an increase in the maximum inflection point before the focus, causing a greater exaggeration in the prediction of the thermal lens effect. Several values of α were investigated from a variety of literature sources including Hale et al. and Kou et al.[18, 19, 23] The smallest value for α seemed to fit the single beam z-scan more closely, however, α was not the only variable which yielded differences in the modeling results.

Studies investigating the index of refraction at specific temperatures for water at 1.313 μm could not be found, though Harvey et al.[21] suggests interpolating n(T) from Schiebener et al.[20] is a good approximation at 1.313 μm. The interpolation procedure used to approximate n(T) is heavily dependent on a known value of n at one known temperature to be used as the reference n from which the approximation is made. The approximation was only done for data between 10 and 90 °C at 0.1 MPa. This background index of refraction influenced the intensity of the thermal lensing effect. If the value for dn/dT was held constant, then the modeling result yielded little to no change in the relative intensity. Changes in the polynomial coefficients used to describe the function n(T) in our model as determined from Schiebener et al.[20] data resulted in over or under predicting the thermal lensing effect as the slope of dn/dT increased and decreased respectively.

Changing the value of κ influenced the modeling results as well. Increasing κ by as little as 1% yielded a noticeable decrease in the peak inflection point before the focus. The value of κ used in this study was taken from the CRC Handbook for water at 298 K.[22] Future thermal lensing models may need to consider $\kappa(T)$.

As a result of the sensitivity of the first order model to α, κ and dn/dT, the conclusion was made to not use the model to find dn/dT by fitting to the data. Since the modeling results indicated the trends of over exaggerating the thermal lensing effect for thicker samples as well as for longer exposure durations, the selection of variables like κ and α could become more important for the long term goal of developing a model to handle thick samples like where strong thermal lensing effects occur such as in the human eye. Instead, further investigation into the selection and sensitivity of the model to α and κ will be done for future models.

Given the trends seen in Fig's. 4 and 5 of the model fitting lower power and thinner sample cases more closely, one would predict the case for the 2 mm thick sample at 2.83 mW would give the best fit. Unfortunately, the results from the single beam z-scan data at lower powers (Fig. 4a) were inherently noisy making the determination of the quality of the fit difficult. Further data collection for lower powers needs to be conducted in future studies.

Preliminary experimental data indicate the first-order model is not an appropriate approximation for thermal lensing for thick sample cases with strong thermal lensing effects. It is likely the aberrations generated in the thermal lens experiment actually break the assumption of a parabolic distribution for n(r) as described in Eq. 11. Higher order models are under current investigation. However, the experiment needs to be repeated under reduced noise levels within the instrumentation to see if sensitivity to lower power levels can be achieved to more accurately test the limitations of the first order model.

REFERENCES

1. ANSI Z136.1-2000. *American National Standard for Safe Use of Lasers*. Laser Institute of America, 2000.

2. Burumcek, E., A. Mudun, C. Karacorlus, and M.O. Arslan. *Laser photocoagulation for persistent serous central retinopathy: results of long-term follow-up*. Ophthalmology, 1997. **104**(12): p 616-622.

3. Le, D. and R. Murphy. *Laser treatment of diabetic macular edema*. Seminars in Ophthalmology, 1994. **9**(1): p. 2-9.

4. Thomas, R., G. Buffington, D. Gavin, L. Irvin, M. Edwards, C. Cain, K. Schuster, J. Stolarski, D. Stolarski, and B. Rockwell. *Experimental and theoretical studies of broadband and optical thermal damage to the retina*. Proceedings of SPIE, 2005. **5688**: p. 411-422.

5. Sliney, D. and D. Freund. *Dependence of retinal model temperature calculations on beam shape and absorption coefficients*. Lasers in Life Sciences. **8**: p. 229-247.

6. Franko, M., and C. D. Tran. *Analytical thermal lens instrumentation*. Review of Scientific Instruments, 1996. **67**(1): p. 1-18.

7. Yariv, A. Quantum Electronics, 3rd Ed. New York, NY, John Wiley and Sons. 1989. p. 106-123.

8. Gordon, J. P., R. C. Leite, R. S. Moore, S. P. Porto, and J. R. Whinnery. *Long transient effects of lasers with inserted liquid samples*. Journal of Applied Physics, 1965. **36**(3): p. 3-8.

9. St. John, W. D., B. Taheri, J. P. Wicksted, R. C. Powell, D. H. Blackburn and D. C. Cranmer. *Time-dependent thermal lensing in lead oxide-modified silicate glass*. Journal of the Optical Society of America B, 1992. **9**(4): p. 610-616.

10. Fang, H. L., and R. L. Swafford. *Analysis of the thermal lensing effect for an optically thick-sample – A revised model*. Journal of Applied Physics, 1979. **50**(11): p. 6609-6615.

11. Kovsh, D., D. Hagan, and E. Van Stryland. *Numerical modeling of thermal refraction in liquids in the transient regime*. Optics Express, 1999. **4**(8).

12. Thomas, R., C. Cain, G. Noojin, D. Stolarski, D. Buffington, L. Irvin, M. Edwards and B. Rockwell. *Extension of thermal damage models of the retina to multi-wavelength sources*. Laser Institute of America, International Laser Safety Conference, 2005. **448**: p. 77-83.

13. Wyld, H. W. Mathematical Methods for Physics. Reading, MA, W. A. Benjamin, Inc. 1976. p. 319-326.

14. Belanger, P. *Beam propagation and the ABCD ray matrices*. Optics Letters, 1991. 16(4): p. 196-198.

15. Harris, J. M. and N. J. Dovichi. *Thermal lens calorimetry*. Analytical Chemistry, 1980. **52**(6): p. 695A-706A.

16. Motamedi, M., A. J. Welch, W. Cheong, S. A. Ghaffari, and O. T. Tan. *Thermal lensing in biological medium*. IEEE Journal of Quantum Electronics, 1988. **24**(4): p. 693-696.

17. Venkatesh, S., S. Guthrie, F. R. Cruickshank, R. T. Bailey, W. S. Foulds and W. R. Lee. *Thermal lens measurements in the cornea*. British Journal of Ophthalmology, 1985. **69**: p. 92-95.

18. Hale, G. and M. Querry. *Optical constants of water in the 200nm to 200μm wavelength region*. Journal of Applied Optics, 1973. **12**: p. 555-563.

19. Kou, L., D. Labrie and P. Chylek. *Refractive indices of water and ice in the 0.65- to 2.5-μm spectral range*. Journal of Applied Optics, 1993. **32**(19): p. 3531-3540.

20. Schiebener, P., J. Straub, J. Levelt Sengers and J. Gallagher. *Refractive index of water and steam as a function of wavelength, temperature and density*. Journal of Physical and Chemical Reference Data, 1990. **19**(3): p. 677-717.

21. Harvey, A., J. Gallagher and J. Levelt Sengers. *Revised formulation for the refractive index of water and steam as a function of wavelength, temperature and density*. Journal of Physical and Chemical Reference Data, 1998. **27**(4): p.761-774.

22. Lide, D. CRC Handbook of Chemistry and Physics: A Ready-Reference Book of Chemical and Physical Data, 83rd Ed. CRC Press, New York. 2002. p. 10-222.

23. Prahl, S. "Optical absorption of water." Oregon Medical Laser Center. 11 May, 1998. http://omlc.ogi.edu/spectra/water/data/hale73.dat